Active Sensing for Data Quality Improvement in Model Learning

Olga Napolitano, Marco Cognetti, Lucia Pallottino, Paolo Salaris, Dimitrios Kanoulas, Valerio Modugno

Active Sensing for Data Quality Improvement in Model Learning

Olga Napolitano[1], Marco Cognetti[2,3], Lucia Pallottino[1], Paolo Salaris[1], Dimitrios Kanoulas[4], Valerio Modugno[4]

***Abstract*— In the application of machine learning to robotics, the quality of data assumes a pivotal role. Many methods use exploration algorithms to select the more informative data points for the model. Nevertheless, these approaches overlook the detrimental influence of measurement errors that invariably impact the data. This paper proposes a novel method to improve the quality of datasets employed in model learning by optimizing metrics based on the combination of exploration and active sensing measures. We use metrics based on a Gaussian Process covariance matrix as exploration metrics, with the aim of letting the system to explore the state space regions where the model uncertainty is higher. We combine it with an active sensing metric based on a norm of the Continuous Riccati Equation optimized to reduce the negative effect of measurement noise on the data. To prove the validity and versatility of our approach, we tested it in a simulation scenario on a unicycle and a quadruped robot.**

I. INTRODUCTION

In the field of machine learning (ML), many researchers dedicate their efforts to the development of powerful models to process large and complicated datasets to make better predictions. However, there has been limited effort to improve the quality of the data, which greatly influences how well ML systems perform [1], especially in real-world applications where the noises and uncertainties that affect the data are not negligible [2].

Data quality also plays a crucial role in ML applications in robotics. The significance of this is especially pronounced in model training. Due to strict online time constraints, fewer data points can be used to provide a timely prediction. Therefore, it is essential to identify a subset of data that is meaningful for the learning process [3]. Consequently, strategies aimed at the selection of data points that maximize information gain are becoming popular. This is done with the expectation that the learned model will achieve the best prediction performance. In [4], the information-theoretic approach for optimal experimental design (OED) is exploited to select the best training data set for explaining the behavior of an unknown system modeled through a Gaussian Process. In the same line, [5] presents an exploration algorithm that maximizes the information acquired at each step quantified by the Fisher information matrix, resulting in an adaptive exploration strategy that can seamlessly interface with diverse parametric learning models. In [6], the authors present a method for multi-agent exploration of spatially distributed physical phenomena based on the maximization of the predicted uncertainty provided by Gaussian Processes. A different approach is taken in [7], where the proposed exploration strategy chooses exploratory actions based on the estimated uncertainty in the learned dynamics model. In [8], an information-cost stochastic nonlinear optimal controller is described, that facilitates the exploration of unknown residual dynamics while safety is guaranteed. Instead, the authors of [9] propose an exploration strategy, where a task-dependent metric that measures the parameters' uncertainty is optimized.

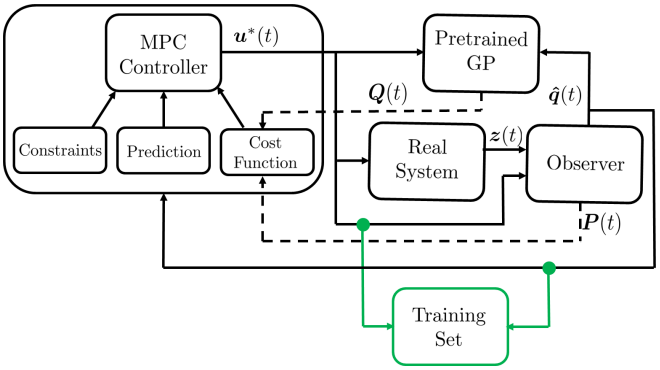

Fig. 1. Control system block diagram of the proposed methodology.

The above-mentioned methodologies focus on the construction of a training set that effectively minimizes the *epistemic error*. Another factor that negatively affects the data quality is the *measurement error* that, in the robotic field, comes from noisy sensor readings. A possible solution is the introduction of an estimator, that will make the learning model process more robust by reducing the negative effects of the measurement noise. However, this is not the best solution, since the estimator passively tries to mitigate this problem. Some approaches – named active sensing/perception control strategy [10] – started to face this problem actively, by finding the optimal control inputs for the robot that minimize the effects of the noise. To the best of our knowledge, while active sensing control is widely used in many robotics scenarios, its application aimed at reducing

[1] Research Center "E. Piaggio" and Dip. of Information Engineering, University of Pisa, Italy. olga.napolitano@phd.unipi.it {paolo.salaris,lucia.pallottino}@unipi.it

[2] LAAS-CNRS, Université de Toulouse, CNRS, Toulouse, France, mcognetti@laas.fr

[3] Université Toulouse III - Paul Sabatier, Toulouse, France.

[4] RPL Lab, University College London, London, United Kingdom.{v.modugno,d.kanoulas}@ucl.ac.uk

This work was supported by the UKRI Future Leaders Fellowship [MR/V025333/1] (RoboHike) and the CDT for Foundational Artificial Intelligence.

measurement error in the active construction of a dataset has been barely explored in the literature.

In this paper, we present a novel methodology for enhancing data quality in the context of model learning, based on the introduction of an active sensing component within an exploration algorithm to reduce both the epistemic and the measurement errors. We introduce novel metrics defined as combinations of exploration and active sensing measures, which are maximized inside a Model Predictive Control (MPC) scheme (see Fig. 1). Regarding the exploration, we considered two metrics: (i) the predicted covariance matrix, named $\boldsymbol{Q}(t)$ in Fig. 1, of a Gaussian Process that is pre-trained on a small dataset; (ii) the *Exploration Gramian*, which quantifies the evolution of the system model uncertainty along a planned trajectory. For the active perception, the chosen metric is a norm of the solution of the Continous Riccati Equation (CRE) – as in [11] – and provided by the Extended Kalman Filter (EKF), chosen as the estimator in this work. To validate the efficacy of our method, we conduct a comparative analysis against a pure exploration algorithm that neglects the impact of measurement noise on the sensor readings. To show the effectiveness of our approach, we tested it on a simulated unicycle and a quadrupedal robot.

The paper is structured as follows. In Section II, some preliminaries about the optimization metrics are introduced. Section III describes the optimal control problem focusing on the combination of metrics regarding active sensing and exploration. In Section IV, the case studies chosen to test our approach are described, while the obtained results are presented in Section V. The paper ends with conclusions and future developments in Section VI.

II. PRELIMINARIES

Let us consider the following nonlinear system

$$\dot{\boldsymbol{q}}(t) = \boldsymbol{f}_n(\boldsymbol{q}(t), \boldsymbol{u}(t)) + \boldsymbol{f}_u(\boldsymbol{q}(t), \boldsymbol{u}(t)) + \boldsymbol{w} \tag{1}$$

$$\boldsymbol{z}(t) = \boldsymbol{h}(\boldsymbol{q}(t)) + \boldsymbol{\nu} \tag{2}$$

where $\boldsymbol{q}(t) \in \mathbb{R}^n$ represents the state of the system, $\boldsymbol{u}(t) \in \mathbb{R}^m$ is the control inputs, $\boldsymbol{z}(t) \in \mathbb{R}^p$ represents the sensor outputs (i.e., the measurements available through sensors at time t), $\boldsymbol{f}_n(\cdot)$ is the known part of the model dynamics. Moreover, $\boldsymbol{f}_u(\cdot) \sim \mathcal{GP}(\boldsymbol{\mu}(t), \boldsymbol{Q}(t))$ is the unknown part of the system dynamics, that is modeled as a Gaussian Process with $\boldsymbol{\mu}(t)$ mean and $\boldsymbol{Q}(t)$ covariance. Finally, $\boldsymbol{h}(\cdot)$ represents the sensor model, and $\boldsymbol{\nu}(t) \sim \mathcal{N}(\boldsymbol{0}, \boldsymbol{R})$ and $\boldsymbol{w}(t) \sim \mathcal{N}(\boldsymbol{0}, \boldsymbol{\Sigma})$, are white, normally-distributed Gaussian noises with zero means and covariance matrices $\boldsymbol{R}$ and $\boldsymbol{\Sigma}$, respectively.

The goal of this paper is to propose a methodology for data quality improvement in model learning by introducing an Active Sensing control strategy in the motions' generation used for the data points collection. The tools used to implement our method are briefly summarized below.

A. Gaussian Processes and exploration measures

Gaussian Processes (GPs) are widely used for system dynamics identification. A generic GP j is a collection of random variables, any finite number of which has a joint Gaussian distribution [12]. Given the following training set

$$\mathcal{D} := \left\{ \boldsymbol{X} := [\boldsymbol{x}_1, \dots, \boldsymbol{x}_N]^\top,\ \boldsymbol{y}^j := \left[y_1^j, \dots, y_N^j\right]^\top \right\} \tag{3}$$

where $\boldsymbol{x}_i$ is an input vector, while the output is given by $y_i^j = g^j(\boldsymbol{x}_i) + w_i$ with $g^j : \mathbb{R}^{\mathcal{D}} \to \mathbb{R}$ and Gaussian noise $w_i \sim \mathcal{N}(0, \sigma_w^2)$, the GP is specified by

$$m^j(\boldsymbol{x}) = \mathbb{E}\left[g^j(\boldsymbol{x})\right]$$
$$k^j(\boldsymbol{x}, \boldsymbol{x}') = \mathbb{E}\left[\left(g^j(\boldsymbol{x}) - m^j(\boldsymbol{x})\right)\left(g^j(\boldsymbol{x}') - m^j(\boldsymbol{x}')\right)^\top\right]$$

where $m^j(\boldsymbol{x})$ is the mean value and $k^j(\boldsymbol{x}, \boldsymbol{x}')$ is the covariance kernel. Then for a function $g^j(\boldsymbol{x})$ the GP can be written as

$$g^j(\boldsymbol{x}) \sim \mathcal{GP}(m^j(\boldsymbol{x}), k^j(\boldsymbol{x}, \boldsymbol{x}')).$$

In this work, we model $\boldsymbol{f}_u(\cdot)$ as a stack of GPs where the total mean $\boldsymbol{\mu}(t)$ and covariance $\boldsymbol{Q}(t)$ are computed as follows:

$$\boldsymbol{\mu}(t) = [m^1(\boldsymbol{x}), \dots, m^n(\boldsymbol{x})]$$
$$\boldsymbol{Q}(t) = diag(k^1(\boldsymbol{x}, \boldsymbol{x}'), \dots, k^n(\boldsymbol{x}, \boldsymbol{x}'))$$

Since the GP models the unknown dynamics $\boldsymbol{f}_u(\cdot) \sim \mathcal{GP}(\boldsymbol{\mu}(t), \boldsymbol{Q}(t))$, the j-th diagonal element of $\boldsymbol{Q}(t)$ describes the uncertainty associated to the j-th component of the unknown dynamics. In other words, the greater the uncertainty of the j-th component, the less explored are the regions of state space associated with it. Consequently, the maximization of (a norm of) $\boldsymbol{Q}(t)$ will drive the robot to explore these regions, hence reducing the corresponding uncertainty.

Let us now compute the explicit form of eq. (1), which is

$$\boldsymbol{q}(t) = \boldsymbol{\Phi}(t, t_0)\boldsymbol{q}_0 + \int_{t_0}^{t} \boldsymbol{\Phi}(t, \tau)\left(\bar{f}(\boldsymbol{q}(t), \boldsymbol{u}(t)) + \tilde{f}(\boldsymbol{q}(t), \boldsymbol{u}(t))\right) \mathrm{d}\tau. \tag{4}$$

where $t > t_0$ and $\boldsymbol{\Phi}(t, t_0)$ is the *system state transition matrix* solution of the following differential equation [13]

$$\dot{\boldsymbol{\Phi}}(t, t_0) = \boldsymbol{A}(t)\boldsymbol{\Phi}(t, t_0), \qquad \boldsymbol{\Phi}(t_0, t_0) = \boldsymbol{I} \tag{5}$$

with $\boldsymbol{A}(t) = \frac{\partial \boldsymbol{f}_n(\boldsymbol{q}(t), \boldsymbol{u}(t))}{\partial \boldsymbol{q}(t)}$.

The first and the second moments of eq. (4) are

$$\boldsymbol{\mu}_q(t) = \boldsymbol{\Phi}(t, t_0)\boldsymbol{q}_0 + \int_{t_0}^{t} \boldsymbol{\Phi}(t, \tau)\left(\bar{f}(\boldsymbol{q}(t), \boldsymbol{u}(t)) + \boldsymbol{\mu}(t)\right) \mathrm{d}\tau, \tag{6}$$

$$\boldsymbol{Q}_q(t) = \int_{t_0}^{t} \boldsymbol{\Phi}(t, \tau)\boldsymbol{Q}(\tau)\boldsymbol{\Phi}^\top(t, \tau)\mathrm{d}\tau. \tag{7}$$

From eq. (7), we then define the *Exploration Gramian* (EG) as follow:

$$\boldsymbol{\mathcal{G}}_{\text{exp}}(t_0, t_{\text{f}}) = \int_{t_0}^{t_{\text{f}}} \boldsymbol{\Phi}(t_{\text{f}}, \tau)\boldsymbol{Q}(\tau)\boldsymbol{\Phi}^\top(t_{\text{f}}, \tau)\mathrm{d}\tau \tag{8}$$

which represents the evolution of the model uncertainty between t_0 and $t_{\text{f}} > t_0$. Therefore, the maximization of

(some norm of) the EG will move the system to collect data in the state space regions with the maximum model uncertainty, allowing the system to explore novel state space regions.

Moreover, eq. (8) can be formulated as a Sylvester differential equation:

$$\dot{\boldsymbol{X}}(t) = \boldsymbol{X}(t)\boldsymbol{A}^\top(t) + \boldsymbol{A}(t)\boldsymbol{X}(t) + \boldsymbol{Q}(t). \tag{9}$$

Indeed, by explicating eq. (9) it follows

$$\boldsymbol{X}(t) = \boldsymbol{\Phi}(t,t_0)\boldsymbol{X}_0\boldsymbol{\Phi}^\top(t,t_0) + \int_{t_0}^{t} \boldsymbol{\Phi}(t,\tau)\boldsymbol{Q}(\tau)\boldsymbol{\Phi}^\top(t,\tau)\mathrm{d}\tau,$$
$$\boldsymbol{X}(t_0) = \boldsymbol{X_0}$$

and hence

$$\boldsymbol{X}(t) = \boldsymbol{\mathcal{G}}_{\text{exp}}(-\infty, t). \tag{10}$$

Thus, by combining eqs. (9) and (10), the final formulation of the EG can be introduced as follows

$$\boldsymbol{\mathcal{G}}_{\text{exp}}(t) = \boldsymbol{\mathcal{G}}_{\text{exp}}(t)\boldsymbol{A}^\top(t) + \boldsymbol{A}(t)\boldsymbol{\mathcal{G}}_{\text{exp}}(t) + \boldsymbol{Q}(t). \tag{11}$$

Equation (11) is obtained by linearizing system (1)–(2) around a nominal trajectory $\boldsymbol{q}(t)$ and neglecting the unknown part $\boldsymbol{f}_u(\cdot)$ and process noise $\boldsymbol{w}(t)$. Finally, an approach for implementing an exploration algorithm can consist of the maximization of (some norm of) the GP covariance matrix $\boldsymbol{Q}(t)$ which model the uncertainty of the unknown dynamic. Alternatively, the maximization of the $\boldsymbol{\mathcal{G}}_{\text{exp}}(t)$ can be used.

In general, the training set in eq. (3) is built during real experiments exploiting sensor readings that might be extremely noisy and hence adversely affect the learning of the model. Therefore, an estimator – e.g., an Extended Kalman Filter as in this work – is needed, and an Active Sensing control strategy must be also introduced to improve the estimator performance.

B. Active Sensing and sensory information measure

The issue of developing optimal control strategies for maximizing the quantity of information collected by the sensors is known as active sensing/perception control, or optimal information gathering. This novel paradigm is gaining significance in various domains of robotics, including aerial [14], [15], multi-agent [16]), and underwater [17] robotics. A crucial aspect in this context is the selection of an appropriate measure for the optimization.

In the scientific domain, numerous information metrics have been introduced, inspired by various theoretical bases such as entropy [18], Bayesian optimization techniques [19], and Fisher's information matrix [20]. Moreover, as introduced in [13] and [21], another suitable metric for quantifying the amount of information – provided by the robot sensors along a trajectory – about the final state $\boldsymbol{q}(t_\text{f})$, is given by the *Constructibility Gramian* (CG) [22], defined as

$$\boldsymbol{\mathcal{G}}_\text{c}(t_0, t_\text{f}) \triangleq \int_{t_0}^{t_\text{f}} \boldsymbol{\Phi}^\top(\tau, t_\text{f})\boldsymbol{H}^\top(\tau)\boldsymbol{W}_\text{c}(\tau)\boldsymbol{H}(\tau)\boldsymbol{\Phi}(\tau, t_\text{f})\,\mathrm{d}\tau\,, \tag{12}$$

where $t_\text{f} > t_0$, $\boldsymbol{H}(\tau) = \frac{\partial \boldsymbol{h}(\boldsymbol{q}(\tau))}{\partial \boldsymbol{q}(\tau)}$, and $\boldsymbol{W}_\text{c}(\tau) \in \mathbb{R}^{p\times p}$ is a symmetric positive definite weight matrix (a design parameter), that may be used for, e.g., accounting for outputs with different units and different uncertainties.

The CG is also related to the covariance matrix of the estimation error $\boldsymbol{P}$ defined as

$$\begin{aligned}\dot{\boldsymbol{P}}(t) = \boldsymbol{P}(t)\boldsymbol{A}(t)^\top + \boldsymbol{A}(t)\boldsymbol{P}(t) - \\ \boldsymbol{P}(t)\boldsymbol{H}^\top(t)\boldsymbol{R}^{-1}\boldsymbol{H}(t)\boldsymbol{P}(t) + \boldsymbol{\Sigma}.\end{aligned} \tag{13}$$

Equation (13) is linked to the linear time-varying system obtained by linearizing system (1)–(2) around a nominal trajectory $\boldsymbol{q}(t)$ and neglecting the unknown part $\boldsymbol{f}_u(\cdot)$.

By exploiting the following link $\dot{\boldsymbol{P}} = -\boldsymbol{P}^{-1}\dot{\boldsymbol{P}}\boldsymbol{P}^{-1}$ and neglecting the process noise covariance matrix $\boldsymbol{\Sigma}$, eq. (13) becomes

$$\dot{\boldsymbol{P}}(t)^{-1} = -\boldsymbol{P}(t)^{-1}\boldsymbol{A}(t) - \boldsymbol{A}(t)^\top\boldsymbol{P}(t)^{-1} + \boldsymbol{H}^\top(t)\boldsymbol{R}^{-1}\boldsymbol{H}(t). \tag{14}$$

By explicating eq. (14) and for $\boldsymbol{P}(t_0) = \boldsymbol{P_0}$ it follows

$$\begin{aligned}\boldsymbol{P}(t)^{-1} = \boldsymbol{\Phi}^{-\top}(t,t_0)\boldsymbol{P}_0\boldsymbol{\Phi}^{-1}(t,t_0) + \\ \int_{t_0}^{t} \boldsymbol{\Phi}^{-\top}(t,\tau)\boldsymbol{H}^\top(\tau)\boldsymbol{R}^{-1}\boldsymbol{H}(\tau)\boldsymbol{\Phi}^{-1}(t,\tau)\mathrm{d}\tau\end{aligned}$$

and hence

$$\boldsymbol{P}^{-1}(t) = \boldsymbol{\mathcal{G}}_\text{c}(-\infty, t). \tag{15}$$

with $\boldsymbol{W}_\text{c}(\tau) = \boldsymbol{R}^{-1}$. Thus, maximizing (a certain norm of) the CG $\boldsymbol{\mathcal{G}}_\text{c}$ is equivalent to minimizing (a certain norm of) the covariance matrix $\boldsymbol{P}$, resulting in a reduction of the estimation uncertainty. It is worth pointing out that eq. (15) holds if the actuation/process noise is neglected. Otherwise, a more complete measure that quantifies both the information from sensors and the degrading effect of the actuation/process noise is (a norm of) $\boldsymbol{P}(t)$.

III. PROBLEM FORMULATION

Let us consider the system in eqs. (1)-(2) and an Extended Kalman Filter, built on the nominal system, that provides an estimate $\hat{\boldsymbol{q}}(t)$ of the real system state $\boldsymbol{q}(t)$. Our goal is to design an optimal control problem that drives the system in the state space regions with large model uncertainty (with the aim of reducing it) and, simultaneously, selects the control action that maximizes the amount of information provided by the robot sensors with the goal of improving the estimator performance. Our control problem is formulated as follows:

Problem 1 *For all $t \in [t_0, t_\text{f}]$, find online the optimal control sequence*

$$\begin{aligned}\boldsymbol{u}^*(t) = \max_{\boldsymbol{u}}\, & J(\hat{\boldsymbol{q}}(t), \boldsymbol{u}(t)) \\ & \textit{s.t.} \\ & 1)\ \dot{\hat{\boldsymbol{q}}}(t) = \boldsymbol{f}_n(\hat{\boldsymbol{q}}(t), \boldsymbol{u}(t)) && (16) \\ & 2)\ \underline{\boldsymbol{q}} \le \hat{\boldsymbol{q}}(t) \le \bar{\boldsymbol{q}} && (17) \\ & 4)\ \underline{\boldsymbol{u}} \le \boldsymbol{u}(t) \le \bar{\boldsymbol{u}} && (18) \\ & 5)\ \boldsymbol{c}(\boldsymbol{u}(t), \hat{\boldsymbol{q}}(t)) \le 0 && (19)\end{aligned}$$

where $J(\hat{\boldsymbol{q}}(t), \boldsymbol{u}(t))$ is an optimization metrics based on the tools introduced in Section II, (16) *is the nominal system dynamics,* (17) *are the state constraints,* (18) *are the control*

constraints, while (19) *are other possible constraints as, for example, a constraint on the total energy consumption for the execution of the task or a Lyapunov constraint to better ensure stability.*

A. Optimization Metrics

In Section II, we have shown how it is possible to measure the system uncertainty and the quantity of information collected by the onboard robot sensors. Moreover, we have also introduced a novel measure, the EG, that can be exploited for the implementation of an exploration algorithm. However, it is worth noting that the two elements can exhibit contrasting behaviors. In fact, the main goal of active sensing is to steer the system towards areas where better measurements are expected, thereby improving the estimation quality. Consequently, active sensing will avoid exploring novel regions, since it does not know which kind of information it will be able to gather. Paradoxically, the primary purpose of the exploration component is to discover and investigate these unexplored regions, resulting in the above-mentioned conflict. Hence, different metrics can be defined, depending on which function the robot should focus on.

The first metric that we introduce in this section is

$$J_1(\hat{\boldsymbol{q}}(t), \boldsymbol{u}(t)) = \text{trace}\left(\boldsymbol{Q}(t)\right). \tag{20}$$

This metric takes into account only the exploration part, ignoring the active sensing contribution. By maximizing J_1, the system will tend to explore regions with high uncertainty from an exploration point of view. We will use this metric as a baseline in our simulations (see Section V).

Another metric is the result of the combination of the exploration and the active sensing components, which can be defined as follows

$$J_2(\hat{\boldsymbol{q}}(t), \boldsymbol{u}(t)) = \text{trace}\left(\boldsymbol{Q}(t)\right) + \text{trace}\left(\boldsymbol{P}^{-1}(t)\right). \tag{21}$$

In eq. (21), the traces (i.e., the mean values) of the covariance matrices of the exploration $\boldsymbol{Q}(t)$ and of the active sensing $\boldsymbol{P}^{-1}(t)$ are linearly combined. The maximization of J_2 will result in finding the trajectory that simultaneously leverages the sensor information and explores the regions with high model uncertainty. However, while $\boldsymbol{Q}(t)$ provides the uncertainty about the input-output relationship at each time t without considering how it evolves along the entire robot's planned trajectory, $\boldsymbol{P}^{-1}(t)$ quantifies the sensory information gained along the complete path. This aspect emphasizes the conflicting behavior between the exploration and active sensing parts. Therefore, a better combination may be the following

$$J_3(\hat{\boldsymbol{q}}(t), \boldsymbol{u}(t)) = \text{trace}\left(\boldsymbol{P}^{-1}(t)\right) + \text{trace}\left(\boldsymbol{\mathcal{G}}_{\text{exp}}(t)\right). \tag{22}$$

Unlike J_2, in J_3 both $\boldsymbol{P}^{-1}(t)$ and $\boldsymbol{\mathcal{G}}_{\text{exp}}(t)$ are cumulative functions that quantify the sensory information and the evolution of the model uncertainty along the planned trajectory.

The metrics introduced in this section will be used as objective functions in Problem 1. The obtained results will be compared to show the improvements of the Active Sensing component in the collection of the data for the training set.

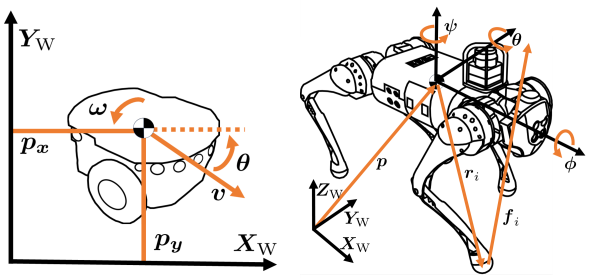

(a) (b)

Fig. 2. Unicycle and quadrupedal robot with their relevant quantities.

IV. CASE STUDIES

In order to prove the validity and versatility of our methodology, we tested it on a simulated unicycle vehicle and a quadrupedal robot. Before delving into the presentation of the two case studies, let us consider system (1), wherein a GP is employed to model errors in $\dot{\boldsymbol{q}}$, the time derivative of the state variable $\boldsymbol{q}$. The training data set for this GP is constructed with input $\boldsymbol{x} = [\boldsymbol{q}, \boldsymbol{u}]$ and output $\boldsymbol{y} = \hat{\dot{\boldsymbol{q}}} - \boldsymbol{f}_n$, where $\hat{\dot{\boldsymbol{q}}}$ represents the estimation of $\dot{\boldsymbol{q}}$. However, an estimator recovers only the state of the system (1). Since we need also $\dot{\boldsymbol{q}}$ for training the GP, an augmentation of the state system becomes necessary.

A. Unicycle vehicle

Let us consider a unicycle vehicle moving on the plane $\boldsymbol{\mathcal{F}}_W = \boldsymbol{X}_W \times \boldsymbol{Y}_W$ (see Fig. 2(a)) and affected by an external disturbance. Its dynamics can be expressed as:

$$\dot{\boldsymbol{q}} = \begin{pmatrix} \cos\theta & 0 \\ \sin\theta & 0 \\ 0 & 1 \end{pmatrix} \boldsymbol{u} + \boldsymbol{f}_u(\boldsymbol{q}, \boldsymbol{u}), \;\; \boldsymbol{f}_n(\boldsymbol{q}, \boldsymbol{u}) = \begin{pmatrix} \cos\theta & 0 \\ \sin\theta & 0 \\ 0 & 1 \end{pmatrix} \tag{23}$$

with $\boldsymbol{q} = [p_x, p_y, \theta]^\top$ the system state and $\boldsymbol{u} = [v, \omega]^\top$ the control input. Moreover, (p_x, p_y) is the robot position w.r.t. $\boldsymbol{\mathcal{F}}_W$, θ is the vehicle yaw, v is the forward velocity, ω is the angular velocity, $\boldsymbol{f}_n(\boldsymbol{q}, \boldsymbol{u})$ is the nominal model and $\boldsymbol{f}_u(\boldsymbol{q}, \boldsymbol{u})$ is a unknown disturbance modeled by a GP. For the purpose of constructing the GP's training set, it is essential to estimate both the linear and angular velocities of the robot. Consequently, it is necessary to reformulate the nominal part in system (23) as follows

$$\dot{\boldsymbol{q}}_{\text{aug}} = \begin{pmatrix} \dot{p}_x \\ \dot{p}_y \\ \dot{\theta} \\ -\sin\theta\omega v + \cos\theta\dot{v} \\ \cos\theta\omega v + \sin\theta\dot{v} \\ \dot{w} \end{pmatrix} \tag{24}$$

with $\boldsymbol{q}_{\text{aug}} = [p_x, p_y, \theta, \dot{p_x}, \dot{p_y}, \dot{\theta}]^\top$ and $\boldsymbol{u}_{\text{aug}} = [v, \omega, \dot{v}, \dot{\omega}]^\top$ as the new state and input vectors, respectively. The new extended nominal system will be used for the prediction in the Problem 1 and in the EKF.

B. Quadrupedal robot

Let us consider a quadrupedal robot as shown in Fig. 2(b). According to [23], its approximate dynamics can be expressed, in the world frame, as follows

$$\frac{d}{dt}\begin{pmatrix}\boldsymbol{p}\\ \boldsymbol{\Theta}\\ \dot{\boldsymbol{p}}\\ \dot{\boldsymbol{\Theta}}\end{pmatrix} = \begin{pmatrix}\mathbf{0}_{3\times3} & \mathbf{0}_{3\times3} & \mathbf{1}_{3\times3} & \mathbf{0}_{3\times3}\\ \mathbf{0}_{3\times3} & \mathbf{0}_{3\times3} & \mathbf{0}_{3\times3} & \boldsymbol{R}(\psi)\\ \mathbf{0}_{3\times3} & \mathbf{0}_{3\times3} & \mathbf{0}_{3\times3} & \mathbf{0}_{3\times3}\\ \mathbf{0}_{3\times3} & \mathbf{0}_{3\times3} & \mathbf{0}_{3\times3} & \mathbf{0}_{3\times3}\end{pmatrix}\begin{pmatrix}\boldsymbol{p}\\ \boldsymbol{\Theta}\\ \dot{\boldsymbol{p}}\\ \dot{\boldsymbol{\Theta}}\end{pmatrix} + \begin{pmatrix}\mathbf{0}_{3\times3} & \dots & \mathbf{0}_{3\times3}\\ \mathbf{0}_{3\times3} & \dots & \mathbf{0}_{3\times3}\\ 1/m & \dots & 1/m\\ \boldsymbol{I}(\psi)^{-1}[\boldsymbol{r}_1]_\times & \dots & \boldsymbol{I}(\psi)^{-1}[\boldsymbol{r}_4]_\times\end{pmatrix}\begin{pmatrix}\boldsymbol{f}_1\\ \vdots\\ \boldsymbol{f}_4\end{pmatrix} + \begin{pmatrix}0\\0\\ \boldsymbol{g}\\0\end{pmatrix} \tag{25}$$

where $\boldsymbol{p}\in\mathbb{R}^3$ is the robot's position, m is the robot's mass, $\boldsymbol{g}\in\mathbb{R}^3$ is the gravity vector and $\boldsymbol{I}\in\mathbb{R}^3$ is the robot's inertia tensor. Moreover, $\Theta=[\phi,\theta,\psi]^\top$ is the robot's orientation where ϕ, θ, and ψ are the roll, pitch, and yaw angles, respectively. Notice that we assumed that the roll and pitch angles do not significantly vary during the robot's motion. Moreover, $\boldsymbol{r}_i\in\mathbb{R}^3$ is the vector connecting the center of mass (CoM) to the point where the force $\boldsymbol{f}_i\in\mathbb{R}^3$ is applied with $i=1\dots4$.

Here, we assume a model mismatch on the CoM linear and angular accelerations of the floating base. Hence, system (1) becomes

$$\dot{\boldsymbol{q}} = \begin{pmatrix}\dot{\boldsymbol{p}}\\ \dot{\boldsymbol{\Theta}}\\ \frac{\sum_{i=1}^4\boldsymbol{f}_i}{m}+\boldsymbol{g}\\ \sum_{i=1}^4\boldsymbol{I}(\psi)\boldsymbol{r}_i\times\boldsymbol{f}_i\end{pmatrix} + \begin{pmatrix}\mathbf{0}_{3\times1}\\ \mathbf{0}_{3\times1}\\ \boldsymbol{f}_u(\boldsymbol{q},\boldsymbol{u})\end{pmatrix},$$
$$\boldsymbol{f}_n(\boldsymbol{q},\boldsymbol{u}) = \begin{pmatrix}\frac{\sum_{i=1}^4\boldsymbol{f}_i}{m}+\boldsymbol{g}\\ \sum_{i=1}^4\boldsymbol{I}(\psi)\boldsymbol{r}_i\times\boldsymbol{f}_i\end{pmatrix}$$

where $\boldsymbol{q}=[\boldsymbol{p},\boldsymbol{\Theta},\dot{\boldsymbol{p}},\dot{\boldsymbol{\Theta}}]^\top$, $\boldsymbol{u}=[\boldsymbol{f}_i,\boldsymbol{r}_i]^\top$ with $i=1\dots4$.

To construct the training set, the CoM accelerations need to be estimated. Therefore, system (25) is extended as follows

$$\frac{d}{dt}\begin{pmatrix}\boldsymbol{p}\\ \boldsymbol{\Theta}\\ \dot{\boldsymbol{p}}\\ \dot{\boldsymbol{\Theta}}\\ \ddot{\boldsymbol{p}}\\ \ddot{\boldsymbol{\Theta}}\end{pmatrix} = \begin{pmatrix}\mathbf{0}_{3\times3} & \mathbf{0}_{3\times3} & \mathbf{1}_{3\times3} & \mathbf{0}_{3\times3} & \mathbf{0}_{3\times3} & \mathbf{0}_{3\times3}\\ \mathbf{0}_{3\times3} & \mathbf{0}_{3\times3} & \mathbf{0}_{3\times3} & \boldsymbol{R}(\psi) & \mathbf{0}_{3\times3} & \mathbf{0}_{3\times3}\\ \mathbf{0}_{3\times3} & \mathbf{0}_{3\times3} & \mathbf{0}_{3\times3} & \mathbf{0}_{3\times3} & \mathbf{1}_{3\times3} & \mathbf{0}_{3\times3}\\ \mathbf{0}_{3\times3} & \mathbf{0}_{3\times3} & \mathbf{0}_{3\times3} & \mathbf{0}_{3\times3} & \mathbf{0}_{3\times3} & \mathbf{1}_{3\times3}\\ \mathbf{0}_{3\times3} & \mathbf{0}_{3\times3} & \mathbf{0}_{3\times3} & \mathbf{0}_{3\times3} & \mathbf{0}_{3\times3} & \mathbf{0}_{3\times3}\\ \mathbf{0}_{3\times3} & \mathbf{0}_{3\times3} & \mathbf{0}_{3\times3} & \mathbf{0}_{3\times3} & \mathbf{0}_{3\times3} & \mathbf{0}_{3\times3}\end{pmatrix}\begin{pmatrix}\boldsymbol{p}\\ \boldsymbol{\Theta}\\ \dot{\boldsymbol{p}}\\ \dot{\boldsymbol{\Theta}}\\ \ddot{\boldsymbol{p}}\\ \ddot{\boldsymbol{\Theta}}\end{pmatrix} + \begin{pmatrix}\mathbf{0}_{3\times3} & \dots & \mathbf{0}_{3\times3}\\ \mathbf{0}_{3\times3} & \dots & \mathbf{0}_{3\times3}\\ \mathbf{0}_{3\times3} & \dots & \mathbf{0}_{3\times3}\\ \mathbf{0}_{3\times3} & \dots & \mathbf{0}_{3\times3}\\ 1/m & \dots & 1/m\\ \boldsymbol{I}(\psi)^{-1}[\boldsymbol{r}_1]_\times & \dots & \boldsymbol{I}(\psi)^{-1}[\boldsymbol{r}_4]_\times\end{pmatrix}\begin{pmatrix}\dot{\boldsymbol{f}}_1\\ \vdots\\ \dot{\boldsymbol{f}}_4\end{pmatrix} \tag{26}$$

where $\boldsymbol{x}=[\boldsymbol{p},\boldsymbol{\Theta},\dot{\boldsymbol{p}},\dot{\boldsymbol{\Theta}},\ddot{\boldsymbol{p}},\ddot{\boldsymbol{\Theta}}]^\top$ is the system's state, $\boldsymbol{u}=\dot{\boldsymbol{f}}_i$ for $i=1\dots4$ is the input and $\boldsymbol{r}_i$ for $i=1\dots4$ is an external parameter. We named the augmented system (26) as Single Rigid Body Dynamic (SRBD) and it will be used for the prediction in the Problem 1 and in the EKF.

V. RESULTS

This section focuses on evaluating the improvement of our method in the training set sample collection of a GP. For each case study, we initially gather the training set samples by individually optimizing each of the objective functions introduced in Section III-A, and then training a GP for each of them, obtaining estimates of the unknown dynamics $\boldsymbol{f}_u$ in eq. (1). In order to test the quality of the reconstructed dynamics, we generated different testing trajectories, also computing the nominal control inputs for tracking them. For each trajectory $(\boldsymbol{q}^{\text{true}},\dot{\boldsymbol{q}}^{\text{true}},\boldsymbol{u})^\top$, we calculated eq. (1) using the reconstructed unknown dynamics $\boldsymbol{f}_u$ by the GP, obtaining $\dot{\boldsymbol{q}}$. Finally, we computed the Root Mean Square (RMS) of the mismatch errors between $\dot{\boldsymbol{q}}^{\text{true}}$ and $\dot{\boldsymbol{q}}$. Finally, Problem 1 is solved with the CasADi tool [24] using the direct single shooting method in an MPC architecture.

A. Unicycle

This section shows the results obtained by testing the proposed approach on the unicycle vehicle case study.

The robot starts form an initial robot configuration $\boldsymbol{q}_0=\mathbf{0}_6$ with zero estimation error and initial uncertainty $\boldsymbol{P}_0=0.4\ \boldsymbol{I}_{6\times6}$. The system is equipped with sensors that provide noisy distances w.r.t. four markers located at $(0,-5)$m, $(0,5)$m, $(10,6)$m, $(-10,-10)$m. We assume the measurement noise covariance matrix $\boldsymbol{R}=0.25\boldsymbol{I}_{4\times4}$ and a process noise with covariance matrix $\boldsymbol{\Sigma}=diag(0.3^2,0.3^2,0.15^2,0.11^2,0.10^2)$. The control input bounds are: -3m/s $\le v\le$ 3m/s and -3rad/s $\le\omega\le$ 3rad/s. We choose a sampling time $\Delta T=0.1$, a prediction horizon $L=10$, and we simulate the unknown true disturbance $\boldsymbol{f}_u(\boldsymbol{q},\boldsymbol{u})$ as

$$\boldsymbol{f}_u(\boldsymbol{q},\boldsymbol{u}) = \begin{pmatrix}-0.3\sin\theta, & 0.3\cos\theta, & 0.3\cos\theta\sin\theta\end{pmatrix}^\top.$$

The goal of the GP is to learn $\bar{\boldsymbol{f}}_u(\boldsymbol{q},\boldsymbol{u})$. We train the GP on a dataset of 200 samples collected every 0.5s. Each sample of the training set consists of the input $\boldsymbol{x}^j=[\hat{p}_x^j,\hat{p}_y^j,\hat{\theta}^j,v^j,\omega^j]^\top$ and the output $\boldsymbol{y}^j=[\hat{p}_x^j,\hat{p}_y^j,\hat{\theta}^j]^\top-\hat{\boldsymbol{f}}_n^j$ where $\hat{\boldsymbol{f}}_n^j=\boldsymbol{f}_n(\hat{\boldsymbol{q}}^j,\boldsymbol{u}^j)$ is the nominal unicycle dynamics evaluated on the estimated state $\hat{\boldsymbol{q}}$ provided by the EKF, and $j=1,\dots,200$. Chosen a testing trajectory $(\boldsymbol{q}^{\text{true}},\dot{\boldsymbol{q}}^{\text{true}},\boldsymbol{u})^\top$, we compute the mismatch error along it as follows:

$$\boldsymbol{e}=\dot{\boldsymbol{q}}^{\text{true}}-\Big(\boldsymbol{f}_n(\boldsymbol{q}^{\text{true}},\boldsymbol{u})+\bar{\boldsymbol{f}}_u(\boldsymbol{q}^{\text{true}},\boldsymbol{u})\Big) \tag{27}$$

with $\boldsymbol{q}^{\text{true}}=[p_x^{\text{true}},p_y^{\text{true}},\theta^{\text{true}}]^\top$, $\dot{\boldsymbol{q}}^{\text{true}}$ its derivative, $\boldsymbol{u}=[v,\omega]$, and $\bar{\boldsymbol{f}}_u(\boldsymbol{q}^{\text{true}})$ is the output of the GP. Since $\dot{\boldsymbol{q}}^{\text{true}}=\boldsymbol{f}_n(\boldsymbol{q}^{\text{true}})+\boldsymbol{f}_u(\boldsymbol{q}^{\text{true}})$, the previous equation reduces to $\boldsymbol{e}=\boldsymbol{f}_u(\boldsymbol{q}^{\text{true}})-\bar{\boldsymbol{f}}_u(\boldsymbol{q}^{\text{true}})$, i.e., the mismatch error. It is important to underline that we compute the error from eq. (27), which does not depend on the knowledge of the unknown dynamics but only on the output of the GP. To assess the quality of the learned models, we compared the RMS of the mismatch errors whose values are shown in TABLE I. Generally, the active sensing component contributes to an enhancement in the quality of the training dataset. Consequently, the RMSE

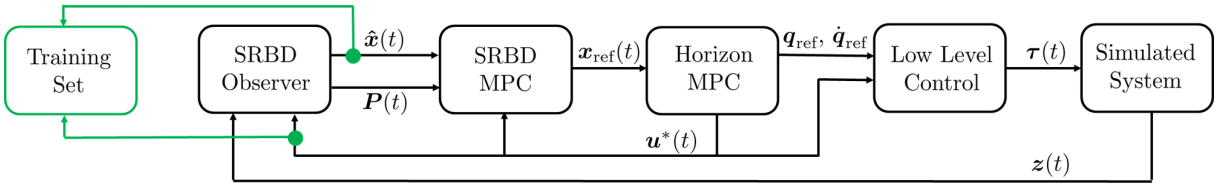

Fig. 3. Control system block diagram for the case study involving the quadrupedal robots.

values for J_2 and J_3 are smaller than those for J_1 (second and third rows vs. the first row in TABLE I). Moreover, the inclusion of the Exploration Gramian (J_3) in place of the covariance matrix $\boldsymbol{Q}$ (J_2) of the GP shows a reduction of the mismatch errors, due to the fact that it optimizes the amount of information related to the exploration over a trajectory rather than on the solely current time (as $\boldsymbol{Q}$ does).

	RMS($\boldsymbol{e}$)	% decrease
J_1	[0.152 0.111 0.080]	–
J_2	[0.141 0.022 0.001]	[-6%, -80%, -99%]
J_3	[0.009 0.011 0.001]	[-94 -90%, -98%]

TABLE I

THE COMPARISON OF THE THREE DIFFERENT OBJECTIVE FUNCTIONS FOR THE UNICYCLE CASE. THE ERROR IN THE TABLE IS DEFINED AS $e = (e_{v_x}, e_{v_y}, e_\omega)^T$, WHERE e_{v_x} (RESP. e_{v_y}) IS THE VELOCITY ERROR ALONG $\boldsymbol{X}_{\text{W}}$ (RESP. $\boldsymbol{Y}_{\text{W}}$) IN THE WORLD FRAME $\boldsymbol{\mathcal{F}}_{\text{W}}$. SIMILARLY, e_ω IS THE ANGULAR VELOCITY ERROR IN THE WORLD FRAME. THE RMS ERROR IS REPORTED IN THE LEFT COLUMN, WHILE THE IMPROVEMENT W.R.T. J_1 (CHOSEN AS BASELINE) IS REPORTED IN THE RIGHT COLUMN IN PERCENTAGE.

B. Quadrupedal Robot

Here, we show the results obtained by testing the proposed methodology on a simulated quadrupedal robot as shown in Fig. 3. At each time instant, an SRBD-MPC solves Problem 1, producing a reference for the robot CoM. Horizon [25] converts the output of SRBD-MPC to references for the robot's motors, which are actuated through PD low-level controllers.

The robot is simulated in PyBullet[1], providing a near-real-world scenario by considering the robot's physics.

For the simulation, we consider $\boldsymbol{q}_0 = \boldsymbol{0}_{18}$ with zero estimation error and initial uncertainty $\boldsymbol{P}_0 = 0.3^2\boldsymbol{I}_{18\times18}$. The system is equipped with an IMU that provides the linear acceleration and the angular velocity of the robot CoM. Additionally, a laser scan that provides noisy distances of the floating base CoM w.r.t. three fixed landmarks located at $(5, 5)$m, $(-5, -2)$m, $(-1, -1)$m. We assume the measurement noise covariance matrix $\boldsymbol{R} = 0.1^2\boldsymbol{I}_{9\times9}$ and a process noise with covariance matrix $\boldsymbol{\Sigma} = 0.5^2\boldsymbol{I}_{18\times18}$. Moreover, we chose the sampling time $\Delta T = 0.04$ s and the prediction horizon $L = 20$.

We trained each GP on a dataset of 200 samples collected every 0.04 s. Each sample of the training set consists of the input $\boldsymbol{x}^j = [\hat{\boldsymbol{p}}^j, \hat{\boldsymbol{\Theta}}^j, \hat{\dot{\boldsymbol{p}}}^j, \hat{\dot{\boldsymbol{\Theta}}}^j, \boldsymbol{f}_i^j, \boldsymbol{r}_i^j]^\top$ and the output $\boldsymbol{y}^j = [\hat{\ddot{\boldsymbol{p}}}^j, \hat{\ddot{\boldsymbol{\Theta}}}^j]^\top - \hat{\boldsymbol{f}}_n(\hat{\boldsymbol{q}}^j, \boldsymbol{u}^j)$ with $\hat{\boldsymbol{q}}$ provided by the EKF, and $j = 1, \ldots, 200$. As for the unicycle, we computed the mismatch error on a testing trajectory as follows:

$$\boldsymbol{e} = \dot{\boldsymbol{q}}^{\text{true}} - \left(\boldsymbol{f}_n(\boldsymbol{q}^{\text{true}}, \boldsymbol{u}) + \bar{\boldsymbol{f}}_u(\boldsymbol{q}^{\text{true}}, \boldsymbol{u})\right)$$

with $\boldsymbol{q}^{\text{true}} = [\boldsymbol{p}^{\text{true}}, \boldsymbol{\Theta}^{\text{true}}]^\top$, $\dot{\boldsymbol{q}}^{\text{true}}$ its derivative, $\boldsymbol{u} = [\boldsymbol{f}_i, \boldsymbol{r}_i]$ with $i = 1, \ldots, 4$, and $\bar{\boldsymbol{f}}_u(\boldsymbol{q}^{\text{true}})$ is the output of the GP. The true trajectories $(\boldsymbol{q}^{\text{true}}, \dot{\boldsymbol{q}}^{\text{true}}, \boldsymbol{u})^\top$ are provided by PyBullet. Since we noticed small variations in the height, roll, and pitch angles of the robot during walking motions, we have excluded these variables from the discussion of the results.

TABLE II shows the comparison between the RMS of mismatch errors. We can observe an overall improvement thanks to the introduction of the active sensing (second and third rows vs the first row in TABLE II). Moreover, the Exploration Gramian confirms, as in the unicycle case, to outperform the other metrics.

	RMS($\boldsymbol{e}$)	%
J_1	[0.867, 0.552, 0.946]	–
J_2	[0.576, 0.419, 0.969]	[-33%, -24%, 2%]
J_3	[0.341, 0.279, 0.706]	[-61%, -49%, -25%]

TABLE II

THE COMPARISON OF THE THREE DIFFERENT OBJECTIVE FUNCTIONS FOR THE QUADRUPED CASE. THE ERROR IN THE TABLE IS DEFINED AS $e = (e_{a_x}, e_{a_z}, e_{a_\psi})^T$, WHERE e_{a_x}, e_{a_y} ARE THE ACCELERATION ERRORS ALONG $\boldsymbol{X}_{\text{W}}$, $\boldsymbol{Y}_{\text{W}}$, RESPECTIVELY. SIMILARLY, e_{a_ψ} IS THE YAW ANGULAR ACCELERATION ERROR. THE RMS ERROR IS REPORTED IN THE LEFT COLUMN, WHILE THE IMPROVEMENT W.R.T. J_1 (CHOSEN AS BASELINE) IS REPORTED IN THE RIGHT COLUMN IN PERCENTAGE.

VI. CONCLUSIONS AND FUTURE WORKS

In this paper, a novel approach that combines an active sensing strategy with an exploration algorithm to improve the quality of a dataset exploited for learning unknown dynamics has been proposed. We tested the validity of our approach through simulations involving two case studies: a unicycle and a quadrupedal robot. We compared the results with a metric that does not consider active sensing in its formulation, showing a data quality improvement using our approach. Future works will aim at implementing our approach in real-time experiments. We are also planning to apply it to different robotic systems (e.g., drones) and integrate it within a control task context.

[1] https://pybullet.org/wordpress/

REFERENCES

[1] L. Budach, M. Feuerpfeil, N. Ihde, A. Nathansen, N. Noack, H. Patzlaff, F. Naumann, and H. Harmouch, "The effects of data quality on machine learning performance," *arXiv preprint arXiv:2207.14529*, 2022.

[2] P. Oliveira, F. Rodrigues, P. R. Henriques, and H. Galhardas, "A taxonomy of data quality problems," 2005.

[3] A. Cully, J. Clune, D. Tarapore, and J.-B. Mouret, "Robots that can adapt like animals," *Nature*, vol. 521, no. 7553, pp. 503–507, 2015.

[4] A. Jain, T. Nghiem, M. Morari, and R. Mangharam, "Learning and control using gaussian processes," in *2018 ACM/IEEE 9th International Conference on Cyber-Physical Systems (ICCPS)*, 2018, pp. 140–149.

[5] M. Blanke and M. Lelarge, "Flex: an adaptive exploration algorithm for nonlinear systems," *arXiv preprint arXiv:2304.13426*, 2023.

[6] A. Viseras, T. Wiedemann, C. Manss, L. Magel, J. Mueller, D. Shutin, and L. Merino, "Decentralized multi-agent exploration with online-learning of gaussian processes," in *2016 IEEE International Conference on Robotics and Automation (ICRA)*, 2016, pp. 4222–4229.

[7] T. M. Moldovan, S. Levine, M. I. Jordan, and P. Abbeel, "Optimism-driven exploration for nonlinear systems," in *2015 IEEE International Conference on Robotics and Automation (ICRA)*, 2015, pp. 3239–3246.

[8] Y. K. Nakka, A. Liu, G. Shi, A. Anandkumar, Y. Yue, and S.-J. Chung, "Chance-constrained trajectory optimization for safe exploration and learning of nonlinear systems," *IEEE Robotics and Automation Letters*, vol. 6, no. 2, pp. 389–396, 2021.

[9] A. Wagenmaker, G. Shi, and K. Jamieson, "Optimal exploration for model-based rl in nonlinear systems," *arXiv preprint arXiv:2306.09210*, 2023.

[10] R. Bajcsy, Y. Aloimonos, and J. Tsotsos, "Revisiting active perception," *Autonomous Robots*, vol. 42, no. 2, pp. 177–196, 2018.

[11] M. Cognetti, P. Salaris, and P. Robuffo Giordano, "Optimal active sensing with process and measurement noise," in *2018 IEEE International Conference on Robotics and Automation (ICRA)*, 2018, pp. 2118–2125.

[12] C. E. Rasmussen and C. K. I. Williams, *Gaussian processes for machine learning.*, ser. Adaptive computation and machine learning. MIT Press, 2006.

[13] P. Salaris, M. Cognetti, R. Spica, and P. R. Giordano, "Online optimal perception-aware trajectory generation," *IEEE Transactions on Robotics*, vol. 35, no. 6, pp. 1307–1322, 2019.

[14] K. Lee, J. Gibson, and E. A. Theodorou, "Aggressive perception-aware navigation using deep optical flow dynamics and pixelmpc," *IEEE Robotics and Automation Letters*, vol. 5, no. 2, pp. 1207–1214, 2020.

[15] M. Samir, C. Assi, S. Sharafeddine, D. Ebrahimi, and A. Ghrayeb, "Age of information aware trajectory planning of uavs in intelligent transportation systems: A deep learning approach," *IEEE Transactions on Vehicular Technology*, vol. 69, no. 11, pp. 12 382–12 395, 2020.

[16] R. Tallamraju, E. Price, R. Ludwig, K. Karlapalem, H. H. Bülthoff, M. J. Black, and A. Ahmad, "Active perception based formation control for multiple aerial vehicles," *IEEE Robotics and Automation Letters*, vol. 4, no. 4, pp. 4491–4498, 2019.

[17] K.-C. Ma, L. Liu, and G. S. Sukhatme, "An information-driven and disturbance-aware planning method for long-term ocean monitoring," in *2016 IEEE/RSJ International Conference on Intelligent Robots and Systems (IROS)*, 2016, pp. 2102–2108.

[18] J. Shan and Q. Sun, "Observability analysis and optimal information gathering of mobile robot navigation system," in *2015 IEEE International Conference on Information and Automation*, 2015, pp. 731–736.

[19] J. Ott, E. Balaban, and M. J. Kochenderfer, "Sequential bayesian optimization for adaptive informative path planning with multimodal sensing," *arXiv preprint arXiv:2209.07660*, 2022.

[20] P. Tokekar, J. Vander Hook, and V. Isler, "Active target localization for bearing based robotic telemetry," in *2011 IEEE/RSJ International Conference on Intelligent Robots and Systems*, 2011, pp. 488–493.

[21] O. Napolitano, D. Fontanelli, L. Pallottino, and P. Salaris, "Gramian-based optimal active sensing control under intermittent measurements," in *2021 IEEE International Conference on Robotics and Automation (ICRA)*, 2021.

[22] P. J. Antsaklis and A. N. Michel, *Linear systems*. Springer Science & Business Media, 2006.

[23] J. Di Carlo, P. M. Wensing, B. Katz, G. Bledt, and S. Kim, "Dynamic locomotion in the mit cheetah 3 through convex model-predictive control," in *2018 IEEE/RSJ International Conference on Intelligent Robots and Systems (IROS)*, 2018, pp. 1–9.

[24] J. Andersson, "A General-Purpose Software Framework for Dynamic Optimization," PhD thesis, Arenberg Doctoral School, KU Leuven, Department of Electrical Engineering (ESAT/SCD) and Optimization in Engineering Center, Kasteelpark Arenberg 10, 3001-Heverlee, Belgium, October 2013.

[25] F. Ruscelli, A. Laurenzi, N. G. Tsagarakis, and E. Mingo Hoffman, "Horizon: A trajectory optimization framework for robotic systems," *Frontiers in Robotics and AI*, vol. 9, p. 899025, 2022.